

# Compliance Maps – A Graphical Tool for Making Structural Comparisons

Gary C. Foss, Boeing Commercial Airplanes, Seattle, Washington

Structural dynamics engineers are frequently asked to make measurements for the purpose of distinguishing differences between two structures or changes within the same structure. A frequent approach is to compare the modal parameters by following a shift in modal frequency or a change in modal assurance criterion between two sets of eigenvectors. The weakness of this approach is that it ignores the total dynamic behavior and focuses only on the eigenvalues and eigenvectors. A graphical method of comparison has been found useful for simple structures. It considers the spatial distribution of the entire frequency response spectrum. A reference line is selected, usually along a structural edge. Point compliances are then measured at short intervals along this line. The compliance is represented by a color scale and plotted against frequency and distance. The result is a three dimensional representation of dynamic behavior along the reference line as a function of position and frequency. Examples show how the technique was used to quickly assess qualitative and quantitative differences between structures.

The most basic normalized response measurement in structural dynamics, and the foundation of experimental modal analysis is the frequency response function (FRF).

$$H_{jk}(\omega) = \frac{X_j}{F_k} \quad (1)$$

This complex ratio represents the forced response of a structure at degree of freedom  $j$  normalized to a force applied at degree of freedom  $k$ . For a generalized structure with multiple degrees of freedom,  $[H]$  is a two dimensional matrix where each element is a frequency response function. It is advantageous for the comparison of structures to consider only the diagonal of this matrix. Each diagonal element is an FRF where excitation and response are measured at the same degree of freedom, commonly called a “drive point” measurement:

$$[H] = \begin{bmatrix} H_{11} & H_{12} & \dots & H_{1k} \\ H_{21} & H_{22} & \dots & H_{2k} \\ \dots & \dots & \dots & \dots \\ H_{k1} & H_{k2} & \dots & H_{kk} \end{bmatrix} \quad (2)$$

If these degrees of freedom are measured along a structural feature that is important to dynamic performance, a three dimensional map can be constructed showing measured amplitudes and frequencies of the FRFs as they vary with position. This can be displayed as a ‘waterfall’ diagram or color map.

## Types of FRFs

Motion can also be expressed as acceleration or velocity. For modal analysis, the most common form of the FRF is the normalized acceleration response, or ‘accelerance.’<sup>1</sup>

$$A(\omega) = \frac{A}{F} \quad (3)$$

The inverse of this is called the “apparent mass.” Sometimes the velocity response is of interest. The velocity FRF is called the ‘mobility.’

$$V(\omega) = \frac{V}{F} \quad (4)$$

The inverse of mobility is called the “mechanical imped-

## Notation

$A(\omega)$ ,  $Y(\omega)$ ,  $H(\omega)$  = acceleration, velocity and displacement frequency response functions (FRFs)  
 $\omega$  = frequency of vibration  
 $A$ ,  $V$ ,  $X$ ,  $F$  = acceleration, velocity, displacement and force spectra

ance.” The displacement response function  $H(\omega)$  is called the “dynamic compliance” or receptance and its inverse is called the “dynamic stiffness.”

$$H(\omega) = \frac{X}{F} \quad (5)$$

The choice of displacement, velocity or acceleration depends on the phenomena of interest. If amplitude and frequency are logarithmically scaled, the choice will affect the average slope of the FRF and hence scaling relative to frequency. Since the measurements are typically made with an accelerometer, acceleration and apparent mass are the easiest quantities to display. However, displacement, stiffness and compliance are more useful and intuitive quantities for comparing structures whose performance depends on resistance to displacement, such as tooling and fixturing used in manufacturing processes.

The left side of Figure 1 shows an accelerance waterfall diagram created by measuring drive point FRFs along the edge of a free-free slender aluminum beam. The  $X$  and  $Y$  axes represent frequency and amplitude. The usual form of a waterfall diagram is to let the  $Z$  direction stacked into the display represent elapsed time. In this case, the  $Z$  direction represents position along the beam and each stacked FRF is a point accelerance spaced every half inch.

As an alternative to the waterfall diagram, the data can be displayed as a color map, shown on the right side of Figure 1. The color scale now represents amplitude and the  $Y$  direction represents physical position. This type of three-dimensional display improves on the waterfall diagram for conceptualizing the spatial as well as spectral nature of structural dynamic behavior. The modes show up as vertical bars of high accelerance (yellow and/or red). The anti-resonance areas are distinguished as dark blue or green valleys of high apparent mass. These features are not distorted or obscured, as they are in the waterfall display on the left. As used here, the term anti-resonance refers to a local minimum in an FRF. A node would be a location where an anti-resonance intersects with a mode frequency, indicating no motion at that location for the mode.

Since benefits are obtained from considering the total dynamic behavior, the FRF magnitudes should usually be scaled logarithmically. This displays the FRF peaks and dips with equal symmetry. For compliance color maps, this means opposite colors equally represent extremes of stiffness or compliance. The choice of colors is arbitrary – for the scale above deep red would equal large accelerance and deep blue would represent large apparent mass.

Viewing data in this way offers an appreciation for how the dynamic properties distribute themselves both spectrally and spatially. The peaks of accelerance line up at constant frequency and vary only in amplitude, defining the mode shape along the reference line. For drive point FRFs, every resonance is followed by an anti-resonance. The anti-resonances do not line up at a single frequency. Their frequencies wander with position from the node line at one mode to the node line at the next mode. By counting the node lines at resonance and not-

<sup>1</sup>Based on a paper presented at the 22nd International Modal Analysis conference, IMAC XXII, Dearborn, MI, January 2004.

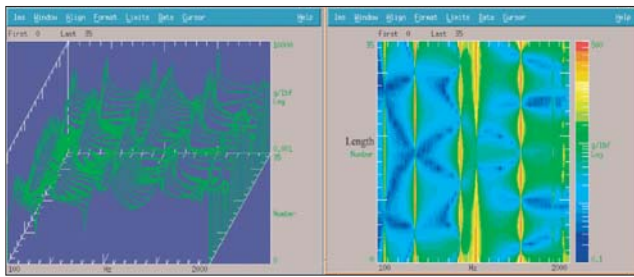


Figure 1. Waterfall plot (left), acceleration (right) along the edge of a free-free slender beam.

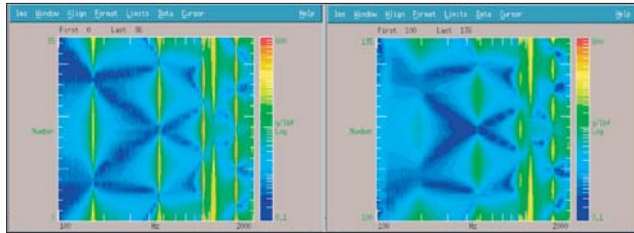


Figure 2. Accelerance comparison of a beam without (left) and with (right) damping treatment. Because the structure is a simple beam, mode shapes can be identified by counting node lines at mode frequencies.

ing their position, the ordering of the shapes for this simple beam is evident. In Figure 1, the first beam bending mode at 170 Hz is obvious with two node lines. The second and third bending modes are at 468 and 918 Hz with three and four node lines respectively. The next mode at 1070 Hz has only one node line and is clearly the first beam torsion mode. A fourth bending mode shows at 1515 Hz with 5 node lines.

Note the characteristic zigzag of the anti-resonance with position. Mode frequencies are global and fixed. Anti-resonances are local and shift frequency with position. At frequencies between the modes, there are certain positions where a force excites almost no response at that frequency.

### Practical Measurement Considerations

For linear, well-behaved structures, impact testing offers a quick and easy path to collect a series of high quality, leakage and alias free FRFs. Structures with unusually high or low damping may present difficulty. For lightly damped structures, the FRF peaks and troughs may span four orders of magnitude (as in Figure 1). Consequently, great care must be taken to optimize the signal to noise ratio for each measurement, which means adjusting the measurement system gain to keep the maximum response level near full scale. High quality, low noise accelerometers are a must to optimize the measurement noise floor.

Another problem is measurement leakage. This may come from several sources. If the structure is lightly damped, it may be difficult to capture the entire response within the measurement time window. In addition, if the test article is suspended free-free, the suspension mode may be a particular problem. In this case, a method of physically suppressing the suspension mode after the structure's flexible modes have disappeared may be needed. Another source of leakage is not allowing enough time for an accelerometer's output to settle after moving it. When an accelerometer is roved from position to position, the physical pressure and body heat from a person's fingers may cause a large DC offset in its output. To avoid leakage, the acquisition should be delayed until this offset bleeds off. Depending on the accelerometer, this may take from a few seconds to several minutes.

An appropriately sized impact hammer should be used which generates a significant voltage at the nominal impact force. In addition to acquisition considerations, the most accurate drive point measurements are obtained when the input and response are measured at the exact same location and direction. This is often not possible. On relatively thin walled



Figure 3. Milling machine with aluminum extrusion clamped on top of fixturing.

structures, it may be possible to excite one side while locating the response transducer directly on the opposite side.

If the structure is heavily damped, the usual trade-off must be made between acquisition length to increase frequency resolution and noisier measurements due to inefficient use of the Fourier transform. If long acquisition times are used relative to the actual response decay time, large portions of the measurement are zero resulting in noisier FRFs. For practical guidance on impact testing, see McConnell<sup>2</sup> and Halvorsen, et al.<sup>3</sup>

For best results with color maps, the FRF measurements should be spaced closely. The number of measured locations sets the resolution of the spatial dimension. If the resolution is too low, a staircase effect occurs due to the data being discrete. Thirty to forty measurements are required to minimize the appearance of this effect. A similar number of discrete color steps should be available in the color scale, for the same reason. Color interpolation should be used, if available.

**Example 1: Structure with Damping Treatment.** Figure 2 shows a comparison of a free-free beam with and without damping treatment applied. The low damped case is on the left and the heavily damped, treated case is on the right. The dark, high apparent mass areas are similar. The light colored, high accelerance vertical bars (yellow/red lines) representing the modal response are one to two orders of magnitude less in the treated beam shown in the right hand figure.

**Example 2: Tooling Comparison.** A manufacturing group was evaluating methods of holding long aluminum extrusions during machining. They wished to know how three different clamping arrangements would affect the dynamic stiffness of the machined part along the machined surface. Beam dynamics can result in unwanted motion of both the tool and extrusion, which not only shortens the life of the machine spindle but also degrades the surface finish of the part. Figure 3 shows an example of one of these machines. The machined extrusion sits atop the fixture extending into the foreground, and is held with hydraulic dovetail clamps.

Three clamping arrangements were tested: (1) a dovetail, (2) a straight section with single clamp, and (3) a straight section with double clamps. The dovetail method is currently used in production but adds cost due to extra material supplied on the raw extrusion to form the dovetail. Figure 4 shows compliance maps of the three arrangements. The top map illustrates the dovetail, the middle map illustrates the single clamp, and the bottom map illustrates the double clamp. The red and yellow areas are the most compliant and the green and blue areas are the most stiff. In judging the effectiveness of the clamping alternatives, the double clamp appears to be the most stiff at the lower frequencies where cutting tooth rates would likely excite undesirable dynamics. Note that all three maps get darker towards the right, indicating increased stiffness. This is because the mass at high frequencies creates a high apparent stiffness, regardless of the clamping arrangement. The darkest ar-

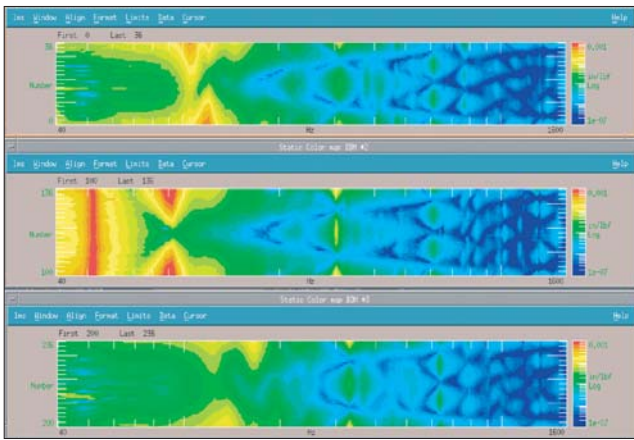


Figure 4. Compliance maps of wing spar mill fixturing alternatives.

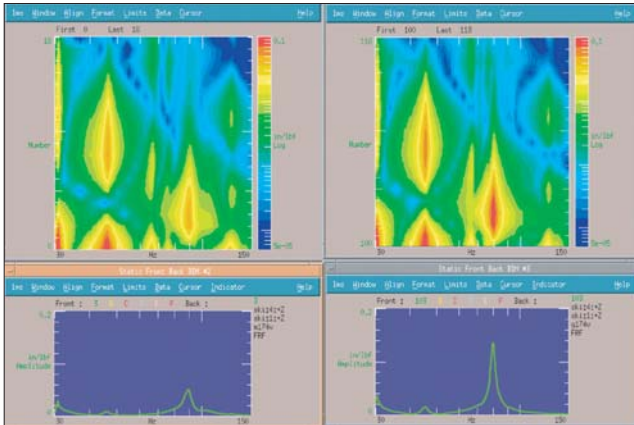


Figure 5. Comparison of different ski constructions. A racing ski is represented on the left and an ordinary ski is represented on the right.

reas here approach 10 million pounds per inch. This illustrates the benefits of operating at high spindle speeds.

**Example 3: Ski Construction.** A manufacturer of skis has been studying the effect of various laminated ski constructions on the ski's dynamic behavior. Skis have been found to behave better under high speed racing conditions if they have thin layers of high strength aluminum in the lay-up. Figure 5 shows compliance maps comparing a laminated racing ski containing two layers of aluminum (left) with a consumer ski made without the aluminum (right). The skis were attached to a fixed cantilever boot through a binding. Drive point FRFs were measured along the edge of the ski from the boot binding to the ski tip and converted to units of compliance. The light areas are very soft and the dark areas are very stiff.

Field testing has shown that the dynamic property most responsible for adverse ski behavior is the torsion mode. Torsional vibration of the ski forebody directly affects edge control and stability, particularly during turns. At first glance, the two color maps appear similar. Note, however, that the torsion mode at 80 Hz is about two and a half times as compliant for the consumer ski as for the racing ski, illustrated by the FRF sections shown below each map. These are sections near the tip of each ski where torsional amplitude is highest.

In general, compliance maps with logarithmic amplitude scaling are best for a panoramic view of the total dynamic behavior. However, the panoramic view may conceal small but important distinctions. In this case, the response at the torsion mode is known to be important. Figure 6 shows the same compliance map comparisons as displayed in Figure 5 with linear amplitude and zoomed in on the torsion mode area. The difference between dynamic behaviors in Figure 6 is much more evident. These data suggested an explanation for what ski racers have always reported – laminated skis with layers of metal and glass may feel quieter than ordinary fiberglass skis because of lower torsional compliance.

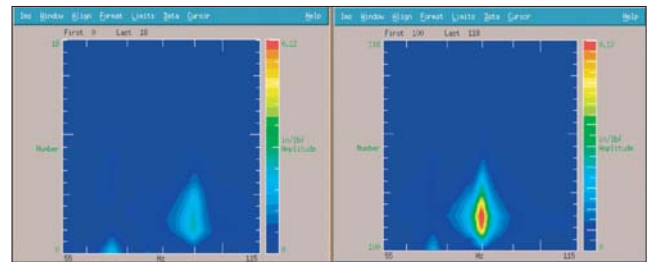


Figure 6. Comparison of ski constructions, highlighting the torsion mode around 80 Hz with a linear color scale.

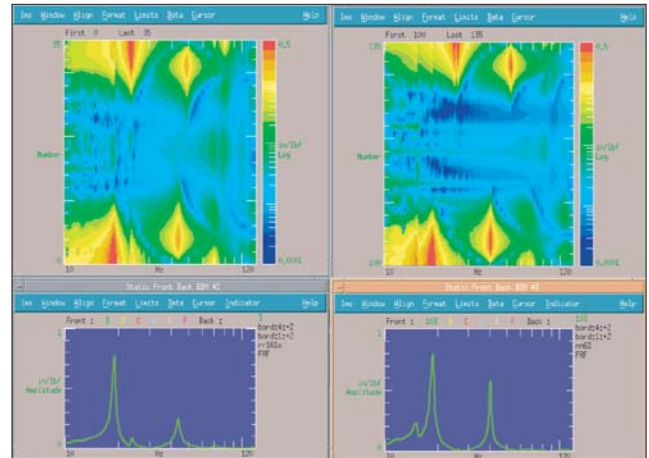


Figure 7. Snowboard construction differences.

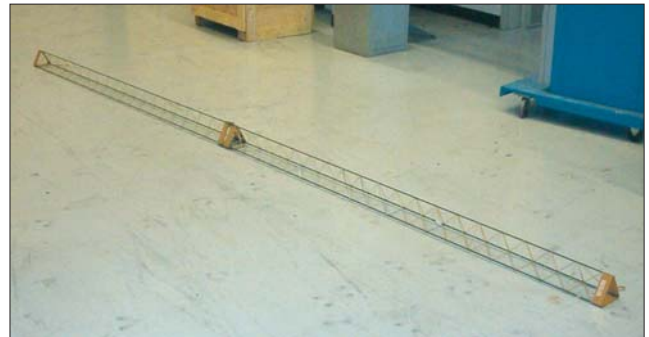


Figure 8. Truss structure. During testing, the truss was suspended from soft springs.

**Example 4: Snowboards.** The same manufacturer of the skis in example 3 wished to use this technique as a tool to quickly evaluate several candidate snowboard constructions. Two snowboards were located that users consistently identified as a “good board” and a “bad board.” The boards were mounted to boots, which were mass filled to approximate the weight of human legs, and suspended free-free from the weighted boots. A reference line was drawn along one edge from tip to tail, and drive point FRFs were measured at 37 locations along it. Figure 7 shows a comparison of the two boards.

A major difference is quickly seen between the two boards by the dark, high stiffness area at low frequencies distinguishing the board on the right. The FRF plots below the maps illustrate slices through the compliance map taken at the snow contact point (front of the board) and show prominently the bending and torsion modes, which are decoupled from the back of the board due to mass loading of the weighted boots.

**Example 5: Damage Detection.** A truss structure was tested to examine the effects on the compliance map when part of the truss was damaged or weakened. The triangular truss was made of graphite composite longitudinal members and adhesively bonded fiberglass interconnect members. It was about 4 inches on a side, 20 feet long, and consisted of 38 sections with a hinge and preloaded latch in the middle so it folds in half for storage. Figure 8 shows a photograph of the truss structure.

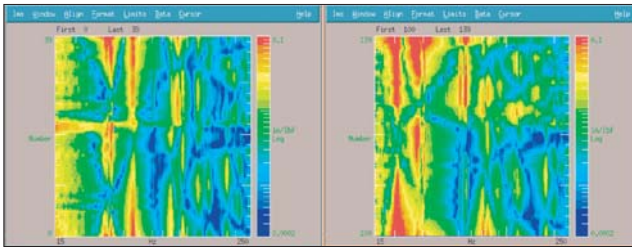


Figure 9. Compliance map of truss structure. The intact truss is on the left; the weakened truss is on the right.

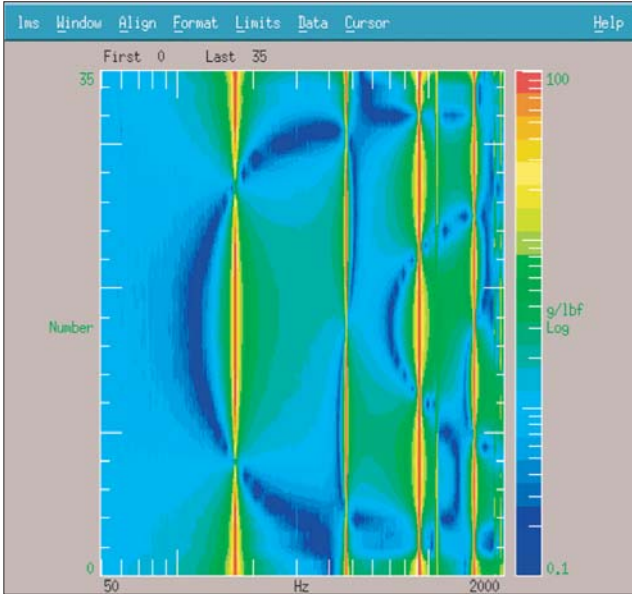


Figure 10. Transfer compliance map of free-free beam along edge to fixed response at center.

Drive point FRFs were measured on the free-free structure at each interconnect node along one of the longitudinal members. Two configurations were tested. The complete truss was tested as a baseline. Another test was performed in which eight out of a total of 118 members were removed. The choice of missing members was dictated by previous uses of the truss. The missing members were concentrated on the right half of the truss. Figure 9 shows compliance maps for both configurations – the complete truss is shown on the left, and the truss with missing interconnect members on the right.

With the removal of the interconnect members, the truss is greatly weakened in torsion. The torsion mode drops from 45

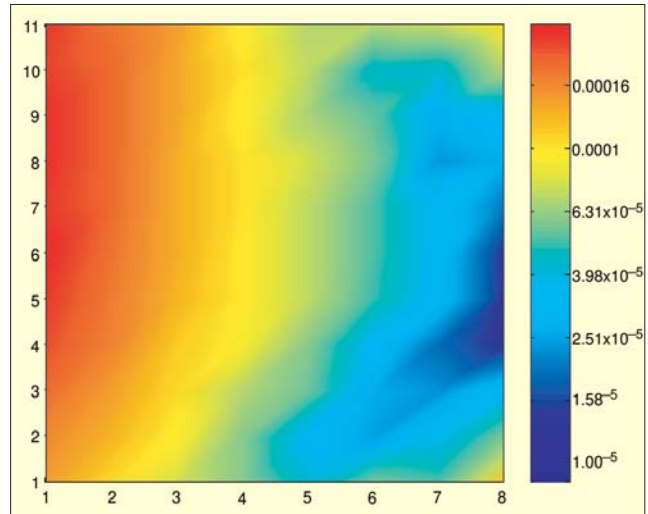


Figure 11. Compliance map of drill press worktable in two spatial dimensions (X and Y) with 80 Hz excitation.

Hz on the left to about 20 Hz on the right. Also note that the upper half of the undamaged truss on the left has a very different topography. It is generally darker than the corresponding portion of the map for the damaged truss on the right. This reflects higher compliance (or lower stiffness) where some structural members are missing. This technique might be applied for damage detection or health testing of civil engineering structures such as bridges. The drive point FRFs could be efficiently measured with a portable impact testing system.

**Example 6: Baseball Bat.** See sidebar.

### Other Compliance Maps

The compliance colormaps shown so far have been composed specifically of drive point FRFs. It may also be useful to consider measurements other than drive points. In this case, a row or column of  $H(\omega)$  can be used to characterize a transfer compliance at a single location on a structure due to excitation elsewhere.

$$[H] = \begin{bmatrix} H_{11} & H_{12} & \dots & H_{1k} \\ H_{21} & H_{22} & \dots & H_{2k} \\ \dots & \dots & \dots & \dots \\ H_{k1} & H_{k2} & \dots & H_{kk} \end{bmatrix} \text{ or } [H] = \begin{bmatrix} H_{11} & H_{12} & \dots & H_{1k} \\ H_{21} & H_{22} & \dots & H_{2k} \\ \dots & \dots & \dots & \dots \\ H_{k1} & H_{k2} & \dots & H_{kk} \end{bmatrix} \quad (6)$$

In this case, either the response or the excitation would be held in a single location of interest while the other roves from point to point. Figure 10 illustrates this on the same beam as

Table 1. MATLAB code for producing color maps.

<code>max_freq = 1024;</code>	% maximum acquisition frequency
<code>blocksize = 1024;</code>	% acquisition number of time points
<code>start_position = 0;</code>	% location of first measurement on structure
<code>end_position = 50;</code>	% location of end measurement on structure
<code>n = 65;</code>	% number of measurements (equally spaced)
<code>x = linspace(0, max_freq, blocksize/2);</code>	% frequency axis
<code>y = linspace(start_position, end_position, n);</code>	% spatial axis
<code>pcolor(x,y,log10(c))</code>	% create colormap
<code>shading interp</code>	% interpolates between colors, makes the plot "smooth"
<code>xlabel('frequency')</code>	% add label to y axis
<code>ylabel('position')</code>	% add label to x axis
<code>h = colorbar;</code>	% change the colorbar to match the data
<code>labels = get(h, 'YTickLabel');</code>	% establish z axis (color) values, keep track of the object handle
<code>labels = str2num(labels);</code>	% get the colorbar y tick labels
<code>labels = 10.^labels;</code>	% convert labels to numbers
	% convert back to data values (not log values)
	% create a cell array of new label strings
<code>for k = 1:length(labels)</code>	
<code>new_labels{k} = num2str(labels(k));</code>	
<code>end</code>	
<code>set(h, 'YTickLabel', new_labels)</code>	% set the new labels back to the object

## Baseball Bat Dynamics

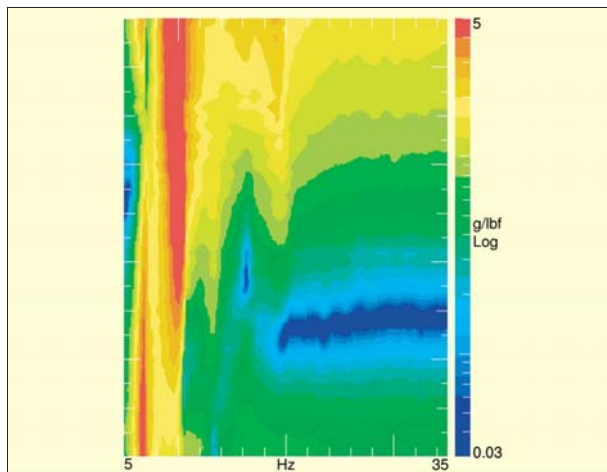


Figure 12. Low frequency acceleration map of the bat. Color units are g/lbf. Each horizontal division is 1.25 inches along the bat, with the tip of the bat at the right and the inside end of the gripping tape at the left.

The structural simplicity of a baseball bat lends itself well to graphical analysis using compliance and acceleration maps. Dynamic properties plotted along the major dimension reveal some interesting (and visually appealing) features.

A 5 ounce baseball travels from the pitcher to the plate in about one half second, traveling 90 mph. It is struck with a 32 ounce bat traveling 70 mph in the other direction. They are in contact for less than 1 millisecond, during which a force of about 9000 pounds compresses the ball to about half its original diameter. Rebounding from the bat, the ball heads for the outfield at about 100 mph.<sup>1</sup>

For the ball to reach the grandstands, it must receive an optimum amount of energy from its collision with the bat. The maximum energy is transferred to the ball when (1) no energy is lost changing the bat's angular momentum and (2) no energy is given up exciting vibration modes of the bat. (Hitting the ball at the correct angle to the bat is a third consideration.)

Condition 1 is met if the ball impacts the bat at the "center of percussion" (COP) defined by  $D = I_0/S_0$ , where:  $D$  = distance from the rotational axis of the bat to the COP;  $I_0$  = mass moment of inertia about the axis of rotation,  $\int r^2 dm$ ; and  $S_0$  = first mass moment about the axis of rotation,  $\int r dm$ . The COP is the point at which the moment of the impact force about the center of gravity causes bat rotation around a stationary point at the batter's hands. If the ball strikes any other point on the bat, the batter's hands will feel a reaction shock. If the reaction shock is high enough, it can be painful, and is sometimes enough to break the bat. With an impact at the COP, the batter's hands feel no net forces. This is one of the bat's "sweet spots."

The COP can be identified by softly suspending the bat and developing a transfer acceleration map using impact

shown in Figure 2. The accelerometer was placed in the exact center of the beam while the hammer was moved to make 36 measurements along the edge of the beam's length. The first four bending modes are obvious, indicated by the yellow/red lines. As expected, the anti-resonance pattern is very different from that shown in Figure 2. In addition, the torsion mode is missing completely because the accelerometer was always located on the torsion mode node line.

### 2-D Spatial Maps

If it is desired to represent two spatial dimensions rather than one, a spectral slice at a single frequency may be taken to pro-

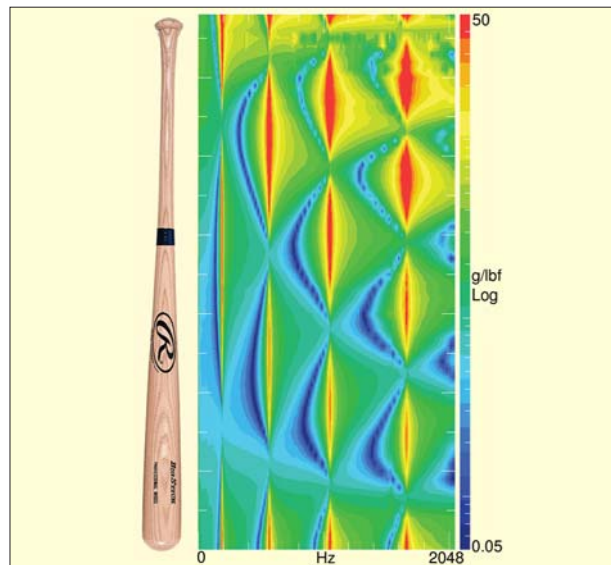


Figure 13. High frequency acceleration map. A bat is shown along the length axis for reference. First, second, third and fourth bending modes are evident as red high response areas lined up horizontally. These are interspersed with blue or green node lines, where each mode is dynamically 'dead.'

testing along the bat's length with a fixed reference accelerometer placed at the assumed axis of rotation (the middle of the handle). One such map is shown in Figure 12. The bat was supported at each end by soft airsprings. The modes indicated by red areas at 6.5 and 9 Hz are the translation and rotation rigid body modes. The broad blue antiresonance at the right locates the COP at about 7 inches from the end of the bat.

Condition 2 is met when the ball impacts the bat near the node lines of vibration. Due to the energy spectrum of the impact force, the first and second bending modes of a wooden bat possess most of the vibrational energy. Fortunately for the batter, the node lines for these modes are close together and the other "sweet spot" of the bat is usually taken as a compromise point halfway between the two node lines for first and second bending.

Figure 13 shows a map of a bat's bending modes, developed using point accelerances from impact testing. Shown on the map are the first, second, third and fourth bending modes.

The "sweet spot" for this wooden bat is really a "sweet area" extending from the first bending node at 7.5 inches to the second bending node at about 6 inches from the tip. The center of percussion is within this area also at about 7 inches. Within this impact area, the batter will feel no sting in his hands from vibration or reaction force, and the hit is most likely to disappear into the stands.

1. Adair, Robert, *The Physics of Baseball*. 2002, Harper Collins.

duce a plot similar to Figure 11. In this case, a flat drill press table was divided up into a 2-D grid of  $8 \times 11$  measurement points. Drive point compliance at an excitation frequency of 80 Hz (4800 RPM) was measured at each point with its magnitude represented as the color scale. The X and Y dimensions now represent the plane of the table. Once again the red area shows high compliance and the blue area is high stiffness. From the compliance map, it is obvious where the table attaches to the column of the drill press, the location of high stiffness.

For the study of dynamic machining problems, a helpful user interface might be constructed with a 2-D map that would allow a slider control to select the frequency slice. The map

would change color with the slider movement to show the compliance/stiffness at any excitation frequency.


## Conclusions

A visualization tool has been shown for efficiently comparing the dynamic properties of structures. This technique requires the collection of a series of high quality, closely spaced FRFs over some length or area. It permits quick graphical comparisons, allows the identification of mode shapes for simple structures, and offers additional insight on the spatial and spectral distribution of modal parameters and general dynamic behavior.

## Addendum

With the exception of Figure 11, the compliance maps shown in this paper were produced using LMS CADA-X software with the color map option from the static display. The LMS color map has a number of color scales available, including a 22 step color scale, which was selected for the data above. MATLAB™ can also be used to display color maps with the PCOLOR command, however there is no option for logarithmic scaling of the colors. Therefore, the data must be converted to logarithmic values. For example, if  $c$  equals an array of FRFs such that each row represents a spatial position and each column represents a measured frequency, the MATLAB code shown in Table 1 will produce plots similar to the LMS color maps.

## References

1. Ewins, D. J., *Modal Testing: Theory, Practice and Application*, 2nd edition, Research Studies Press, 2000, p. 34.
2. McConnell, K. G., *Vibration Testing: Theory and Practice*, Wiley, 1995, p. 475-501.
3. Halvorsen, W. G., and Brown, D. L., "Impulse Technique for Structural Frequency Response Testing," *Sound and Vibration*, Nov. 1977, pp. 8-21. 

---

The author can be contacted at [gary.c.foss@boeing.com](mailto:gary.c.foss@boeing.com).

MATLAB is a registered trademark of The Mathworks, Inc.